

TruthLens: Explainable DeepFake Detection for Face Manipulated and Fully Synthetic Data

Rohit Kundu^{1,2}, Shan Jia¹, Vishal Mohanty¹, Athula Balachandran¹, Amit K. Roy-Chowdhury²

¹Google LLC, ²University of California, Riverside

{rohit.kundu@email, amitrc@ece}.ucr.edu; {rohitkun, shanjia, vishalmohanty, athula}@google.com

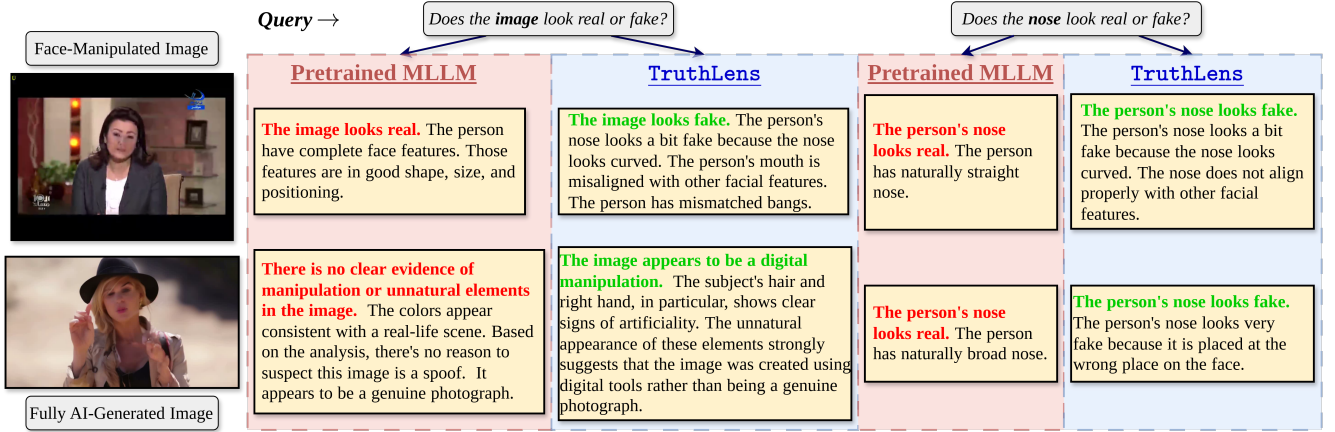


Figure 1. **Illustration of Explanations:** Comparison of explanations generated by the pretrained PaLiGemma2 [53] multimodal large language model (MLLM) and our proposed TruthLens framework on a face-manipulated image (from the FaceForensics++ [47] dataset) and a fully AI-generated image (produced by StableVideoDiffusion [8] and sourced from the DVF [52] dataset). The pretrained MLLM fails to detect subtle inconsistencies in the manipulated images, resulting in incorrect explanations. In contrast, TruthLens provides accurate predictions along with detailed, fine-grained reasoning for the detected manipulations.

Abstract

Detecting DeepFakes has become a crucial research area as the widespread use of AI image generators enables the effortless creation of face-manipulated and fully synthetic content, yet existing methods are often limited to binary classification (real vs. fake) and lack interpretability. To address these challenges, we propose TruthLens, a novel and highly generalizable framework for DeepFake detection that not only determines whether an image is real or fake but also provides detailed textual reasoning for its predictions. Unlike traditional methods, TruthLens effectively handles both face-manipulated DeepFakes and fully AI-generated content while addressing fine-grained queries such as “Does the eyes/nose/mouth look real or fake?”

The architecture of TruthLens combines the global contextual understanding of multimodal large language models like PaliGemma2 with the localized feature extraction capabilities of vision-only models like DINOv2. This hybrid design leverages the complementary strengths of

both models, enabling robust detection of subtle manipulations while maintaining interpretability. Extensive experiments on diverse datasets demonstrate that TruthLens outperforms state-of-the-art methods in detection accuracy (by 2-14%) and explainability, in both in-domain and cross-data settings, generalizing effectively across traditional and emerging manipulation techniques.

1. Introduction

With the advent of synthetic media generation technology [30, 46] hyper-realistic manipulated images can be created with minimal technical knowledge, which can even deceive humans. Until recently, DeepFakes only referred to manipulations of faces [23, 32, 58] using techniques like face-swapping [22, 23, 48] or lip syncing [6, 15, 43]. However, state-of-the-art image-to-video (I2V) and text-to-video (T2V) models [46, 60, 72] enable malicious actors to manipulate beyond faces, generating entire images/videos.

While several DeepFake detection frameworks [14, 29, 54, 64] have been proposed, most of them focus on face-manipulated content and are limited to binary real vs. fake classification. These methods lack explicit, interpretable explanations for their predictions, which is a critical requirement in scenarios requiring human understanding. Explainability fosters trust and transparency in AI systems, making it an essential component of robust DeepFake detection frameworks. Thus, there is a pressing need for a highly generalizable DeepFake detection framework that can effectively handle both traditional face-manipulated content and fully AI-generated media and can go beyond simple binary classification by offering easy-to-understand, human-interpretable results. This would enable accurate detection as well as actionable insights into the nature and location of manipulations, addressing the dual challenges of generalization and explainability in DeepFake detection.

Recently, multimodal large language models (MLLMs) have demonstrated remarkable problem-solving capabilities across diverse tasks [4, 69, 73], driven by their ability to learn powerful multimodal representations. These models hold significant potential for addressing the explainability challenge in DeepFake detection. Some methods [28, 50] have explored leveraging pretrained MLLMs like GPT-4V [1] and Gemini-1.0 [56] for this purpose. However, pretrained MLLMs are typically optimized for general-purpose tasks, such as image captioning [36, 56], visual question answering [12, 13, 31], etc., and lack the domain-specific adaptation required to reliably generate explanations for DeepFake detection [11]. This limitation is evident in our evaluation of the pretrained PaliGemma2 [53] MLLM (example in Fig. 1, results in Table 3), which highlights the need for task-specific fine-tuning to achieve reliable and interpretable outputs in this domain.

To address this challenge, we propose *TruthLens*, a comprehensive DeepFake explainability framework that goes *beyond binary classification to provide detailed textual reasoning* for its predictions. Designed to be highly generalizable, *TruthLens* handles both face-manipulated and fully AI-generated content, answering nuanced queries such as “Does the eyes/nose/mouth look real or fake?” This flexibility enables deeper insights into manipulations, enhancing its utility in diverse scenarios.

Existing DeepFake explainability methods [11, 52, 70] rely solely on fine-tuning Vision-Language Models (VLMs), which often miss subtle manipulations. In face-manipulated images, alterations are confined to small pixel regions, unlike fully synthetic content where the entire frame is manipulated. VLMs can only provide global context [59], so \mathcal{X}^2 -DFD [11] and DD-VQA [70] crop faces as a preprocessing step. However, this approach fails to generalize when full frames need analysis, as in fully synthetic content. Similarly, methods like MM-Det [52] which are

tailored for fully-synthetic content explanation fail to capture localized inconsistencies in face-manipulated data.

To address these limitations, *TruthLens* integrates features from both PaliGemma2 [53] MLLM and DINOv2 [41] vision-only model (VOM). PaliGemma2 provides global context through vision-language capabilities, enabling a holistic image content understanding, while DINOv2 captures localized inconsistencies by extracting fine-grained features from image patches. This hybrid approach ensures comprehensive detection of manipulations by leveraging both global and local feature representations.

The contributions of this work are as follows.

- We propose *TruthLens*, a novel and highly generalizable framework for DeepFake detection. Unlike existing methods that are often restricted to face-manipulated content, *TruthLens* is designed to effectively handle both face-manipulated DeepFakes and fully AI-generated content. This versatility ensures its applicability across a diverse range of DeepFake scenarios, addressing the growing complexity of manipulation techniques.
- *TruthLens* goes beyond simple real vs. fake classification by providing detailed textual reasoning for its predictions. By generating human-readable explanations, *TruthLens* enhances transparency and supports informed decision-making.
- Moving beyond naive MLLM fine-tuning, we design a robust approach where *TruthLens* integrates features from both the PaliGemma2 [53] MLLM and the DINOv2 [41] VOM. This hybrid design leverages the global context provided by the MLLM and the localized detail captured by the VOM, enabling accurate detection of subtle manipulations while maintaining interpretability.
- We show that *TruthLens* generalizes well across traditional face manipulations and fully AI-generated content, outperforming state-of-the-art methods in detection accuracy and explainability across several diverse datasets.

2. Related Work

Conventional DeepFake Detection: Early DeepFake detection methods [33, 68] struggled with generalizability in cross-dataset settings, which is critical for in-the-wild detection. Dong et al. [20] tackled this issue by proposing an ID-unaware model that focuses on local image regions and employs an Artifact Detection Module to reduce identity bias, improving generalization. Similarly, Ojha et al. [40] enhanced generalization by utilizing features from a CLIP [45] model pretrained on large-scale image-text pairs, moving beyond reliance on model-specific artifacts.

Methods like [10, 17, 18, 62] address the synthetic content detection problem. Corvi et al. analyzed spectral [17] and frequency-domain [18] artifacts, such as spectral peaks and autocorrelation patterns, in diffusion-generated images, while Wang et al. [62] proposed DIRE, leveraging recon-

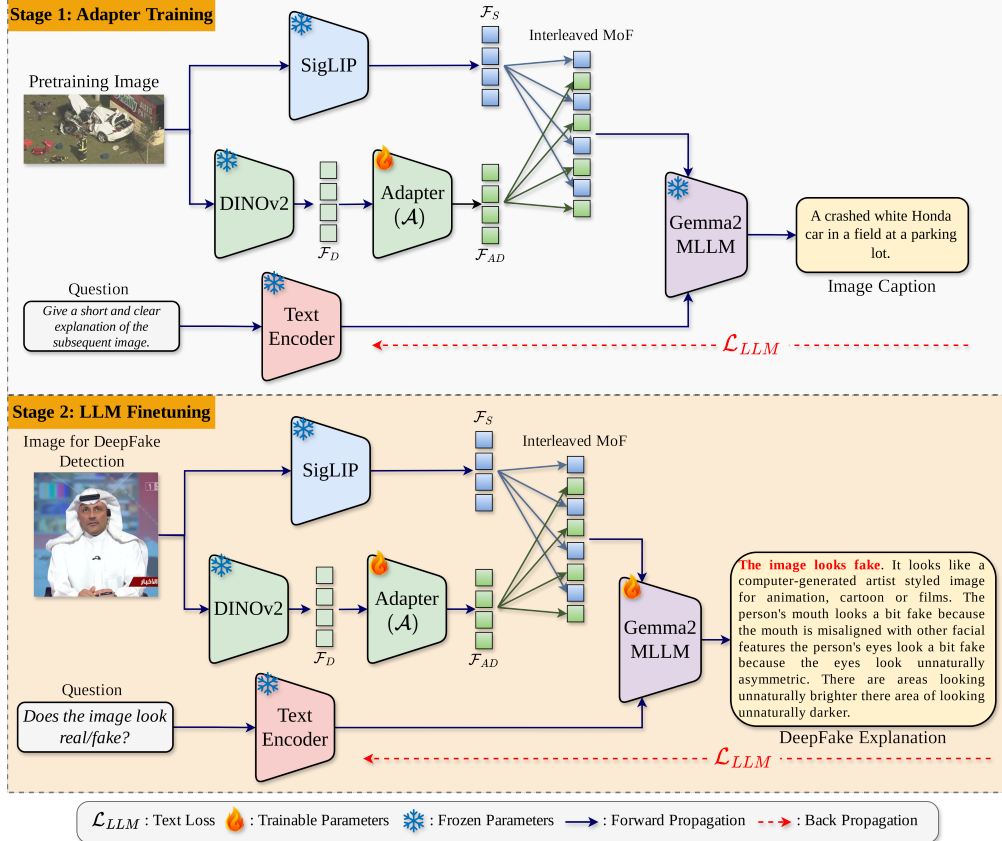


Figure 2. The overall framework for TruthLens utilizes the PaliGemma2 [53] MLLM, which combines the SigLIP-So400m/14 [3] vision encoder and the Gemma2 [57] LLM. Since SigLIP features are already compatible with Gemma2, we directly use them, but DINOv2 features require compatibility adaptation. Thus, in Stage-1 (Sec. 3.4.1), we train an adapter using the LCS-558K [36] image-captioning dataset to align DINOv2 features with Gemma2. In Stage-2 (Sec. 3.4.2), we fine-tune the adapter and Gemma2 LLM with DD-VQA [70] and DVF [52] language annotated datasets, enabling explainable DeepFake detection on both face-manipulated and fully synthetic content.

struction differences from pre-trained diffusion models to distinguish real from synthetic images with strong cross-model generalization. These methods focus on diffusion-generated images, and are not designed to handle the unique challenges of detecting facial DeepFakes. UNITE [29] is the only method that performs DeepFake detection on all types of fake media (face/background manipulated and fully synthetic content) using a transformer architecture with “attention-diversity” loss. However, all of the aforementioned methods are designed only for real vs. fake classification tasks and cannot provide prediction explanations, which we address using TruthLens.

Visual Explainability: Most methods [63, 74] use Grad-CAM analysis for explaining the predictions of DeepFake detectors. However, Grad-CAM is insufficient, because it often highlights irrelevant or coarse regions, lacks fine-grained localization, making it less effective for pinpointing manipulated areas in DeepFake images. Aghasanli et al. [2] used identity-specific features (prototypes) for DeepFake detection, and calculated Euclidean distance of the test images from the prototypes to infer which person’s Deep-

Fake has been created. This method fails in fine-grained localization and relies on identities used in training, making it ineffective for in-the-wild DeepFakes. In contrast, TruthLens provides precise, identity-agnostic explanations by pinpointing manipulated regions, delivering fine-grained reasoning without relying on predefined prototypes.

Text Explainability: Text-based DeepFake explainability provides fine-grained explanations more effectively than visual interpretability methods, as it can leverage natural language to articulate specific inconsistencies or manipulations in the content, offering detailed reasoning that is easier for humans to understand. However, there are very limited methods that integrate natural language with DeepFake Detection. [28, 50] were early attempts that used ChatGPT (GPT-4V [1]) and Gemini-1.0 [56] in zero-shot settings to detect face-manipulated images. DD-VQA [70] finetuned the BLIP VLM [31] to generate text explanations, using their proposed DD-VQA text-annotations dataset (based on FaceForensics++ [47]). Similarly, the \mathcal{X}^2 -DFD framework [11] finetunes the LLaVA model [36] for face-manipulated content explanation. However, all of these methods de-

tected and cropped the faces before analysis, assuming human faces are always visible. Thus, they are not fit for synthetic content detection.

To the best of our knowledge, MM-Det [52] is the only method that attempted explainability in fully AI-generated content (generated by T2V/I2V models), by finetuning the LLaVA model [36] using their proposed DVF dataset. However, this model cannot capture subtle inconsistencies and thus cannot detect face-manipulated data.

Summary of Relation to Existing Work: In the literature, there does not exist a singular model which can provide explanations for both face-manipulated and fully synthetic content. Thus, we propose *TruthLens*, a unified model for DeepFake detection and text-based explanation on any form of manipulated content- whether it’s face-manipulated, or fully AI-generated.

3. Proposed Method

Unlike existing methods [11, 70] that focus solely on face-manipulated DeepFakes, our model provides a unified framework for explainability in both face-manipulated and fully AI-generated images. The problem formulation is detailed in Sec. 3.1. To achieve this unified explainability, we leverage features from PaliGemma2 [53] and DINOv2 [41] (Sec. 3.2) through our Mixture of Features (MoF) approach (Sec. 3.3). Our training strategy is elaborated in Sec. 3.4. Fig. 2 presents the architectural overview of *TruthLens*.

3.1. Problem Setup

Given an image $\mathcal{I} \in \mathbb{R}^{H \times W \times 3}$ and a question \mathcal{Q} related to DeepFake detection, the objective of our model is to generate a detailed answer \mathcal{E} that determines whether the image is real or manipulated and provides an explanation for the decision. Our goal is to find the optimal parameters θ of our model f_θ that minimize the following objective function:

$$\arg \min_{\theta} \sum_{(\mathcal{I}, \mathcal{Q}, \mathcal{E}) \in \mathcal{D}} \mathcal{L}(f_\theta(\mathcal{I}, \mathcal{Q}), \mathcal{E}) \quad (1)$$

where \mathcal{D} is our training dataset of image-question-explanation triplets, and \mathcal{L} is a loss function measuring discrepancy between generated and ground truth explanations. This formulation enables our model to learn accurate, detailed explanations for DeepFake images.

3.2. Foundation Models

DINOv2: DINOv2 [41] is a state-of-the-art vision-only foundation model, designed to learn robust visual features through self-supervised learning. It builds upon the Vision Transformer (ViT) [21] architecture, employing a patch size of 14 pixels to divide input images into non-overlapping patches. Each patch is then processed through the transformer layers to extract localized features. For an input image of size $H \times H$ this results in $H/14 = d$ patches along

each dimension, yielding a total of d^2 tokens. Each token is represented by a feature vector of dimensionality 2048, producing an output tensor of shape $d^2 \times 2048$. For our pipeline, we set the image resolution to 448^2 , yielding,

$$\mathcal{F}_D = \text{DINOv2}(\mathcal{I}^{448 \times 448 \times 3}), \quad (2)$$

where $\mathcal{F}_D \in \mathbb{R}^{1024 \times 2048}$, with 1024 tokens, each with a feature dimension of 2048.

PaliGemma2: PaliGemma2 [53] is a state-of-the-art MLLM designed for vision-language tasks, integrating advanced capabilities in both image and text processing. It employs a two-tower architecture comprising the SigLIP-So400m/14 [3] vision encoder and the Gemma2 [57] language model. The SigLIP encoder can process images at resolutions of 224^2 , 448^2 , or 896^2 , converting them into visual tokens through a ViT [21] architecture. These tokens are linearly projected to align with the Gemma2 input space. Meanwhile, the Gemma2 language model, available in 3B, 10B, and 28B parameter configurations, generates autoregressive text outputs. This design allows PaliGemma2 to combine visual and textual data into a unified multimodal representation for downstream tasks. In our pipeline, the image resolution is 448^2 , and the image tower yields,

$$\mathcal{F}_S = \text{SigLIP}(\mathcal{I}^{448 \times 448 \times 3}), \quad (3)$$

where, $\mathcal{F}_S \in \mathbb{R}^{1024 \times 2304}$, with 1024 tokens, each with a feature dimension of 2304.

3.3. Feature Mixing

In our *TruthLens* pipeline for explainable DeepFake detection, we combine features from both DINOv2 [41] and PaliGemma2 [53] to leverage their complementary strengths in capturing localized and global visual information. DeepFake images, particularly those involving facial manipulations, present unique challenges as only a small region of the image (e.g., the face) is altered, while the majority of the image remains real. VLMs like PaliGemma2 are highly effective at providing global context and aligning visual features with textual explanations, but they often struggle to capture subtle, localized inconsistencies in small regions [59]. Conversely, VOMs like DINOv2 excel at identifying fine-grained pixel-level artifacts in specific areas, making them particularly suited for detecting manipulations in face regions. Since our goal is to have a unified explainable model for detecting both face-manipulated and fully AI-generated, we leverage both of these models.

Since the DINOv2 features are not directly compatible with the Gemma2 [57] tower of PaliGemma2, we design an adapter module (\mathcal{A}) consisting of single MLP layer, as,

$$\mathcal{F}_{AD} = \mathcal{A}(\mathcal{F}_D), \quad (4)$$

where, adapted DINOv2 features $\mathcal{F}_{AD} \in \mathbb{R}^{1024 \times 2304}$, with 1024 tokens, each with a feature dimension of 2304.

In our pipeline for explainable DeepFake detection, we leverage the Mixture of Features (MoF) approach to combine visual representations from PaliGemma2’s vision encoder (SigLIP [3]) and DINOv2 [41], utilizing their complementary strengths to create a richer feature space. SigLIP excels at aligning visual features with textual descriptions, while DINOv2 captures fine-grained visual details and spatial relationships. To integrate these features effectively, we employ two strategies: *interleaving* and *concatenation*. In the interleaving strategy (I-MoF), tokens are alternated between the adapted DINOv2 features and SigLIP features along the token dimension, ensuring a balanced contribution from both models at a fine-grained level. In the concatenation strategy (C-MoF), tokens from both models are concatenated along the token dimension, preserving all information in a unified representation. Both strategies result in a combined feature space of size 2048×2304 , enabling robust performance.

3.4. Training Strategy

Our training pipeline consists of two stages. **Stage-1** involves pretraining the adapter on a general-purpose multimodal alignment task using a large-scale dataset, establishing a foundation for feature extraction and contextual understanding. **Stage-2** focuses on task-specific fine-tuning for DeepFake detection, where both the adapter and the LLM are jointly optimized to capture localized manipulations and DeepFake-specific nuances. This two-stage approach ensures effective generalization across diverse datasets while enabling adaptation to subtle inconsistencies unique to DeepFake content.

Keeping the adapter trainable during Stage-2 is essential for adapting DINOv2 features to task-specific requirements. While Stage-1 pretraining provides general-purpose multimodal alignment, fine-tuning in Stage-2 enables the adapter to better capture localized manipulations relevant to DeepFake detection. Freezing the adapter during Stage-2 results in lower performance (refer to ablation results in supplementary material), likely due to a mismatch between pretrained features and task-specific needs. Joint optimization of both the adapter and LLM ensures robust performance across diverse DeepFake scenarios, including face-manipulated and fully synthetic content.

3.4.1. Stage-1: Adapter Training

In this stage, we train a one-layer DINOv2 adapter module using the LLaVA-Pretrain LCS-558K [36] image-captioning dataset. The adapter module is a lightweight MLP that transforms the DINOv2 features to align with the feature space expected by the Gemma2 LLM. During this training phase, the Gemma2 LLM remains frozen, and only the adapter module is trainable. To train the adapter, we use the Mixture of Features (MoF) approach to combine DINOv2 and SigLIP features for each image in the dataset.

The model is optimized using a cross-entropy loss (\mathcal{L}_{LLM}) over the text tokens generated by the Gemma2 LLM, ensuring that the adapted DINOv2 features contribute meaningfully to text generation.

The LCS-558K dataset [36] is widely used in literature [27, 39, 42] for training adapters in multimodal systems because it provides a large-scale, diverse collection of image-caption pairs. This diversity ensures that the adapter learns to generalize across a wide range of visual concepts and contexts, which is critical for downstream tasks requiring robust visual grounding and textual alignment. Furthermore, training on an image-captioning dataset aligns with the pretraining objectives of vision-language models, enabling effective integration of visual and textual modalities.

We opted against using annotated DeepFake datasets for adapter pretraining to avoid overfitting on specific manipulation patterns. Instead, we pretrain on a diverse image-captioning dataset to ensure that the adapter learns strong foundational representations, which can be fine-tuned for DeepFake detection later. This two-stage approach combines general-purpose pretraining with subsequent task-specific fine-tuning for effective DeepFake explainability.

3.4.2. Stage-2: LLM Finetuning

In this stage, we finetune the LLM of PaliGemma2 [53] (Gemma2-3B [57]) using the Mixture of Features (MoF) vision embeddings and question-answer pairs derived from language-annotated DeepFake datasets. Unlike Stage-1, where the LLM was frozen, both the LLM and the adapter module are trainable in this phase. This joint training enables the model to align visual manipulations, such as subtle facial artifacts or inconsistencies, with textual reasoning, thereby generating accurate and explainable predictions for DeepFake detection.

Tokenization: To train the model, we tokenize the input question and answer using the Gemma2 tokenizer model (τ). Let the input question be denoted as \mathcal{Q} and the corresponding answer as \mathcal{E} . The tokenization is defined as:

$$\text{Prefix Tokens: } \mathcal{T}_{\text{prefix}} = \tau(\mathcal{Q}); \quad (5)$$

$$\text{Separator Token: } \mathcal{T}_{\text{separator}} = \tau("\backslash n"); \quad (6)$$

$$\text{Suffix Tokens: } \mathcal{T}_{\text{suffix}} = \tau(\mathcal{E}). \quad (7)$$

The combined token sequence is constructed as:

$$\mathcal{T} = [\mathcal{T}_{\text{prefix}}, \mathcal{T}_{\text{separator}}, \mathcal{T}_{\text{suffix}}], \quad (8)$$

where $\mathcal{T}_{\text{prefix}}$ represents the question tokens with full attention, $\mathcal{T}_{\text{separator}}$ separates the question and answer, and $\mathcal{T}_{\text{suffix}}$ represents the answer tokens with causal attention.

Loss computation: To compute the cross-entropy loss (\mathcal{L}_{LLM}), we define three masks:

1. **Attention Mask (\mathcal{M}_{at}):** The attention mask is used to control whether a token attends to all previous tokens

(causal attention or 1) or has full attention (0) to all tokens in the sequence. For prefix tokens (question), full attention is applied and for suffix tokens (answer), causal attention is applied. During training, \mathcal{M}_{ar} ensures that:

$$\mathcal{T}_i = f(\mathcal{T}_j) \quad \forall j < i \quad (9)$$

where f represents the model’s attention mechanism, ensuring that each token in the suffix can only attend to previous tokens.

2. **Input Mask (\mathcal{M}_{input}):** Identifies valid tokens (1) versus padding (0). \mathcal{M}_{input} prevents padding tokens from contributing to loss computation or model updates, ensuring only meaningful tokens are processed by the model.
3. **Loss Mask (\mathcal{M}_{loss}):** Specifies which tokens contribute to the loss (1 for suffix tokens, 0 for prefix tokens). \mathcal{M}_{loss} is derived from both \mathcal{M}_{ar} and \mathcal{M}_{input} , ensuring that only valid suffix tokens contribute to the loss.

These masks are defined as:

$$\mathcal{M}_{ar} = [0]^{|\mathcal{T}_{prefix}|+|\mathcal{T}_{separator}|} + [1]^{|\mathcal{T}_{suffix}|}, \quad (10)$$

$$\mathcal{M}_{input} = [1]^{|\mathcal{T}|}, \quad (11)$$

$$\mathcal{M}_{loss} = [0]^{|\mathcal{T}_{prefix}|+|\mathcal{T}_{separator}|} + [1]^{|\mathcal{T}_{suffix}|}. \quad (12)$$

During training, the cross-entropy loss is computed only on the suffix tokens:

$$L_{LLM} = - \frac{\sum_{i=1}^{|\mathcal{T}|} \mathcal{M}_{loss}[i] \cdot \log P(\mathcal{T}[i])}{\sum_{i=1}^{|\mathcal{M}_{loss}|} \mathcal{M}_{loss}[i]}, \quad (13)$$

where $P(\cdot)$ is the predicted probability distribution over tokens.

During testing, only the prefix tokens \mathcal{T}_{prefix} are provided as input, and the model generates predictions autoregressively. The separator and suffix tokens are generated step-by-step based on causal attention.

4. Experiments

Evaluation Metrics: We employ an LLM-as-a-judge mechanism using Gemini-1.0 [56] to evaluate TruthLens’s detection accuracy. Gemini compares the ground truth explanation with TruthLens’s prediction, providing a binary “yes” or “no” output to determine if they reach the same conclusion. This forms our LLM-as-a-judge detection accuracy metric.

Additionally, we assess answer generation quality using standard natural language metrics: BLEU_3, BLEU_4, ROUGE_L, and CIDEr. These metrics evaluate the fluency, coherence, and alignment of generated explanations with ground truth responses. This combined approach ensures a comprehensive assessment of both detection accuracy and explanation quality for TruthLens.

Training Details: TruthLens is trained using Stochastic Gradient Descent (SGD) with an initial learning rate of

Table 1. **SOTA Comparison on Face-Manipulated Data.** The methods used for the comparisons are specifically designed for face-manipulation detection. However our TruthLens framework is designed for both face-manipulated and synthetic content detection. DD-VQA [70] is in-domain evaluation, all the other datasets are cross-data evaluations. **Best** and **second-best** performances are marked.

Dataset	Method	Accuracy \uparrow	BLEU_4 \uparrow	ROUGE_L \uparrow	CIDEr \uparrow
DD-VQA [70]	XceptionNet-BLIP-TI [70]	89.25%	-	-	-
	HifiNet [25]	89.16%	-	-	-
	HifiNet-BLIP-TI [70]	91.25%	-	-	-
	RECCE [9]	91.03%	-	-	-
	RECCE-BLIP [70]	89.22%	-	-	-
	RECCE-BLIP-TI [70]	92.08%	-	-	-
	BLIP [31]	81.68%	0.3569	0.5664	1.8177
	BLIP-T [70]	83.65%	0.3714	0.5774	1.8715
	BLIP-I [70]	84.87%	0.3800	0.5882	1.8931
	BLIP-TI [70]	87.49%	0.4075	0.6085	2.0567
	TruthLens	94.12%	0.4304	0.6285	2.6321
CelebDF [34]	XceptionNet-BLIP-TI [70]	62.41%	-	-	-
	HifiNet [25]	67.20%	-	-	-
	HifiNet-BLIP-TI [70]	69.37%	-	-	-
	RECCE [9]	67.96%	-	-	-
	RECCE-BLIP [70]	68.07%	-	-	-
	RECCE-BLIP-TI [70]	69.46%	-	-	-
	TALL [64]	90.79%	-	-	-
	ISTVT [71]	84.10%	-	-	-
	Choi et al. [16]	89.00%	-	-	-
	TruthLens	92.86%	0.3986	0.5481	2.1045
DF40 [67]	λ^2 -DFD [11]	85.60%	-	-	-
	RECCE [9]	78.10%	-	-	-
	SBI [51]	64.40%	-	-	-
	CORE [38]	76.10%	-	-	-
	IID [26]	75.70%	-	-	-
	UCF [65]	77.50%	-	-	-
	LSDA [66]	77.80%	-	-	-
	CDFA [35]	75.90%	-	-	-
	ProgressiveDet [14]	78.70%	-	-	-
	TruthLens	99.58%	0.4279	0.5338	2.3947

0.0001, scheduled to decay following a cosine annealing schedule. The training process is conducted with a batch size of 64 over 5 epochs for both Stage-1 and Stage-2 training. The framework is implemented in JAX and executed on 8 TPUv3 chips, ensuring efficient large-scale training.

TruthLens is trained on DD-VQA [70] (face-manipulated FaceForensics++ or FF++ [47] data annotated with language, resolution ablation in supplementary) and DVF [52] (fully synthetic data) datasets and evaluated on:

- Face-manipulated datasets: DD-VQA [70], CelebDF [34] and DF40 [67]
- Fully synthetic datasets: DVF [52] and DeMamba [10]

Except for DD-VQA [70] and DVF [52], the other datasets lack language annotations. However, since class labels are available for these datasets and they are only used for evaluation, we manually design the question-answer pairs. Specifically, the questions are framed as “Does the image look real or fake?”, and the corresponding answers are structured as “The image looks <real/fake>.” This ensures consistency in evaluation across all datasets.

State-of-the-art Comparison: TruthLens’s performance is evaluated against state-of-the-art (SOTA) methods for DeepFake detection on face-manipulated data (Table 1) and fully AI-generated data (Table 2). Existing SOTA methods are typically specialized for either face-manipulated or synthetic content detection, lacking the versatility to address both. In contrast, TruthLens is a unified framework that effectively handles both categories.

Despite the more challenging cross-dataset evalua-

Table 2. **SOTA Comparison on Synthetic Data:** The compared methods are trained specifically for synthetic image detection and evaluated in-domain. In contrast, TruthLens is trained on DD-VQA [70] and DVF [52], with DVF as in-domain evaluation and DeMamba [10] as cross-dataset evaluation. Despite this more challenging setup, TruthLens outperforms SOTA methods, including those trained directly on DeMamba. Notably, competitor methods do not report answer generation metrics. **Best** and second-best performances are marked.

Dataset	Method	Accuracy ↑	BLEU.4 ↑	ROUGE.L ↑	CIDEr ↑
DVF [52]	CNNDet [61]	78.20%	-	-	-
	DIRE [62]	62.10%	-	-	-
	Raising [19]	67.00%	-	-	-
	UNI-FD [40]	74.10%	-	-	-
	F3Net [44]	81.30%	-	-	-
	ViViT [5]	79.10%	-	-	-
	TALL [64]	69.50%	-	-	-
	TS2-Net [37]	72.10%	-	-	-
	DE-FAKE [49]	72.10%	-	-	-
	HiFiNet [25]	84.30%	-	-	-
DeMamba [10]	DVF [52]	92.00%	-	-	-
	TruthLens	94.47%	0.4279	0.5338	2.1744
	TALL [64]	88.42%	-	-	-
	F3Net [44]	86.04%	-	-	-
	NPR [55]	83.45%	-	-	-
	STIL [24]	85.35%	-	-	-
	MINTIME-CLIP-B [10]	89.98%	-	-	-
	FTCN-CLIP-B [10]	89.67%	-	-	-
	CLIP-B-PT [10]	41.82%	-	-	-
	DeMamba-CLIP-PT [10]	79.98%	-	-	-
DeMamba [10]	XCLIP-B-PT [10]	65.83%	-	-	-
	DeMamba-XCLIP-PT [10]	79.31%	-	-	-
	XCLIP-B-FT [10]	86.07%	-	-	-
	TruthLens	90.49%	0.4165	0.5121	2.0619

Table 3. **Pretrained vs. Finetuned MLLM:** Performance comparison between pretrained and finetuned PaliGemma2 [53].

Dataset	Finetuned	Accuracy ↑	BLEU.3 ↑	BLEU.4 ↑	ROUGE.L ↑	CIDEr ↑
<i>Face Manipulated Data</i>						
DD-VQA [70]	✗	11.50%	0.0000	0.0000	0.0218	0.2610
	✓	88.19% (+76.69%)	0.4012 (+0.4012)	0.3768 (+0.3768)	0.5633 (+0.5415)	2.1478 (+1.8868)
CelebDF [34]	✗	12.73%	0.0000	0.0000	0.0379	0.2549
	✓	85.38% (+72.65%)	0.3015 (+0.3015)	0.3445 (+0.3445)	0.4852 (+0.4473)	1.5617 (+1.3068)
DF40 [67]	✗	0.32%	0.0000	0.0000	0.0009	0.0064
	✓	73.58% (+73.26%)	0.3031 (+0.3031)	0.3386 (+0.3386)	0.4019 (+0.4010)	1.6198 (+1.6134)
<i>Synthetic Data</i>						
DVF [52]	✗	33.07%	0.0000	0.0000	0.0034	0.0001
	✓	79.88% (+46.81%)	0.3142 (+0.3142)	0.3839 (+0.3839)	0.4877 (+0.4843)	1.8629 (+1.8628)
DeMamba [10]	✗	26.13%	0.0000	0.0000	0.0000	0.0428
	✓	86.81% (+60.68%)	0.3027 (+0.3027)	0.3698 (+0.3698)	0.4892 (+0.4892)	1.6729 (+1.6301)

Table 4. **Ablation on TruthLens Vision Features:** SigLIP features, adapted DINOv2 features, concatenate MoF, and interleave MoF strategies. The results highlight the superior performance of the interleave MoF strategy over other approaches.

Dataset	Features Used	Accuracy ↑	BLEU.3 ↑	BLEU.4 ↑	ROUGE.L ↑	CIDEr ↑
DD-VQA [70]	SigLIP only	88.19%	0.4012	0.3768	0.5633	2.1478
	Adapted DINOv2 only	90.45%	0.4107	0.4143	0.5843	2.0816
	C-MoF	93.56%	0.4497	0.4286	0.6015	2.4193
	I-MoF	94.12%	0.4649	0.4304	0.6285	2.6321
DVF [52]	SigLIP only	79.88%	0.3142	0.3839	0.4877	1.8629
	Adapted DINOv2 only	77.67%	0.3077	0.3786	0.4873	1.7465
	C-MoF	92.81%	0.3614	0.4261	0.5234	2.1605
	I-MoF	94.47%	0.3786	0.4279	0.5338	2.1744

tion setup, TruthLens consistently outperforms existing SOTA methods in both in-domain and cross-dataset evaluations. Notably, on datasets like DeMamba [10], where SOTA methods are trained and tested on the same dataset, TruthLens achieves superior performance without being trained on DeMamba. This highlights its exceptional generalization capability, essential for addressing the diverse and evolving landscape of DeepFake manipulations. Additionally, TruthLens provides detailed textual explanations for its predictions, offering enhanced interpretability.

Table 5. **Adapter Ablations:** Results obtained by the TruthLens model on various adapter settings.

Dataset	Adapter Settings	Accuracy ↑	BLEU.3 ↑	BLEU.4 ↑	ROUGE.L ↑	CIDEr ↑
<i>Face-Manipulated Data</i>						
DD-VQA [70]	Stage-1 trained on DD-VQA [70] & DVF [52]	79.13%	0.3017	0.2975	0.5113	1.5812
	Stage-2 frozen	86.56% (+7.43%)	0.3964 (+0.0947)	0.3897 (+0.0922)	0.5712 (+0.0599)	2.0447 (+0.4635)
	Co-trained with LLM (No pretraining)	90.371% (+3.81%)	0.4107 (+0.0143)	0.4066 (+0.0169)	0.6015 (+0.0303)	2.3186 (+0.2739)
	TruthLens	94.12% (+3.75%)	0.4649 (+0.0542)	0.4304 (+0.0238)	0.6285 (+0.0270)	2.6321 (+0.3135)
CelebDF [34]	Stage-1 trained on DD-VQA [70] & DVF [52]	71.32%	0.2173	0.2617	0.3950	1.2934
	Stage-2 frozen	81.4% (+10.08%)	0.2934 (+0.0761)	0.3315 (+0.0698)	0.5068 (+0.1118)	1.7156 (+0.4222)
	Co-trained with LLM (No pretraining)	88.13% (+6.73%)	0.3185 (+0.0251)	0.3413 (+0.0098)	0.5246 (+0.0178)	1.8221 (+0.1065)
	TruthLens	92.86% (+4.73%)	0.3578 (+0.0393)	0.3986 (+0.0573)	0.5481 (+0.0235)	2.1045 (+0.2824)
DF40 [67]	Stage-1 trained on DD-VQA [70] & DVF [52]	61.32%	0.1521	0.1946	0.3481	0.6835
	Stage-2 frozen	82.71% (+21.39%)	0.2864 (+0.1343)	0.3318 (+0.1372)	0.4259 (+0.0778)	1.3193 (+0.6358)
	Co-trained with LLM (No pretraining)	91.73% (+9.02%)	0.3015 (+0.0151)	0.3716 (+0.0398)	0.4816 (+0.0557)	1.7163 (+0.3970)
	TruthLens	99.58% (+17.85%)	0.3998 (+0.0983)	0.4690 (+0.0974)	0.5395 (+0.0579)	2.3947 (+0.6784)
<i>Synthetic Data</i>						
DVF [52]	Stage-1 trained on DD-VQA [70] & DVF [52]	74.39%	0.2317	0.2815	0.4014	1.0961
	Stage-2 frozen	89.23% (+14.84%)	0.3173 (+0.0856)	0.3681 (+0.0866)	0.4846 (+0.0832)	1.6820 (+0.5859)
	Co-trained with LLM (No pretraining)	92.11% (+2.88%)	0.335 (+0.0177)	0.3875 (+0.0194)	0.4972 (+0.0126)	1.8988 (+0.2168)
	TruthLens	94.47% (+2.36%)	0.3786 (+0.0436)	0.4279 (+0.0404)	0.5338 (+0.0366)	2.1744 (+0.2756)
DeMamba [10]	Stage-1 trained on DD-VQA [70] & DVF [52]	66.25%	0.2315	0.3109	0.4017	1.0416
	Stage-2 frozen	81.79% (+15.54%)	0.3016 (+0.0701)	0.3763 (+0.0654)	0.4368 (+0.0351)	1.5633 (+0.5217)
	Co-trained with LLM (No pretraining)	86.54% (+4.75%)	0.3281 (+0.0265)	0.3865 (+0.0102)	0.4833 (+0.0465)	1.8154 (+0.2521)
	TruthLens	90.49% (+3.95%)	0.3552 (+0.0271)	0.4165 (+0.0300)	0.5121 (+0.0288)	2.0619 (+0.2465)

Qualitative Results: The qualitative results obtained by TruthLens are presented in Fig. 3, demonstrating its capability to provide detailed and accurate explanations for both face-manipulated images from DF40 [67] and fully AI-generated images from DeMamba [10] in cross-dataset settings. For face-manipulated content, TruthLens identifies subtle inconsistencies, such as unnatural textures or irregular lighting, explaining these manipulations with fine-grained reasoning. In fully synthetic content, TruthLens highlights anomalies including overly smooth skin lacking texture, asymmetric facial features, and unnatural lighting effects typical of T2V/I2V-generated imagery.

Notably, even when skin is visible only in small pixel regions of synthetic images, TruthLens successfully infers inconsistencies, showcasing the effectiveness of localized features obtained from DINOv2 [41] embeddings. It also accurately identifies real images, describing natural features like even skin and proper hairstyles. This demonstrates TruthLens’s ability to capture inconsistencies reliably and distinguish between manipulated and authentic content, emphasizing its robustness in detecting diverse manipulation types while offering interpretable insights.

Pretrained vs. Finetuned MLLM: We compare the performance of the pretrained and fine-tuned PaliGemma2 [7] model (without DINOv2 [41] feature mixing) in Table 3. While the pretrained model shows strong general-purpose capabilities, it performs suboptimally for DeepFake explainability. Fine-tuning on domain-specific data significantly improves performance, highlighting the necessity of adapting MLLMs like PaliGemma2 to specialized tasks

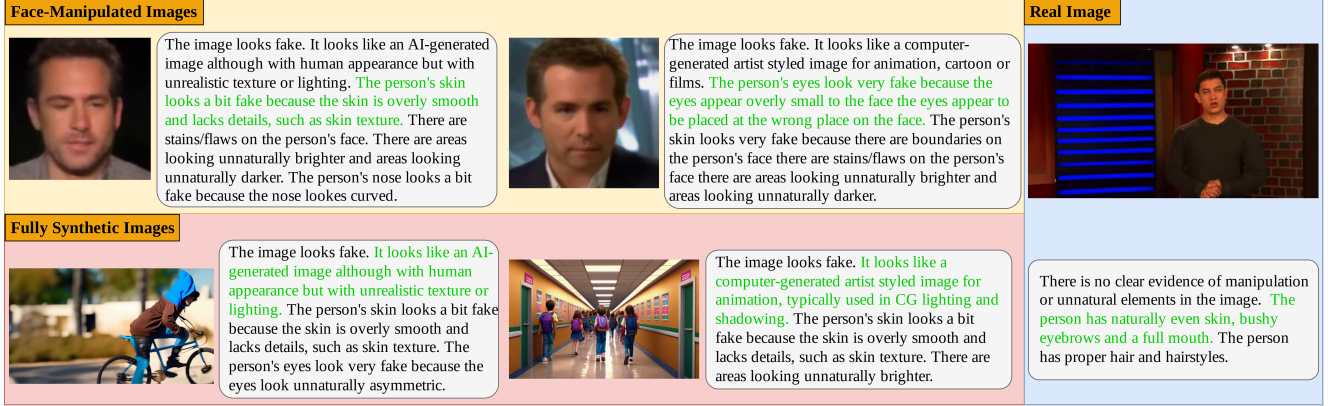


Figure 3. DeepFake explanations obtained by TruthLens in *cross-dataset settings* on face-manipulated images from DF40 [67], fully synthetic images from DeMamba [10] and a real image from CelebDF [34]. The query in all cases is “Does the image look real or fake?”

such as DeepFake detection. Fine-tuning enables the model to better capture task-specific nuances, achieving higher accuracy and alignment with domain requirements.

Ablation study on Feature Mixing: We perform an ablation study to assess the importance of different features and their mixing strategies within TruthLens, as detailed in Table 4, using the DD-VQA [70] and DVF [52] datasets. The results show that using SigLIP or adapted DINOv2 features independently yields suboptimal performance compared to the combined MoF approach. Additionally, the interleave MoF strategy outperforms the concatenate MoF strategy, demonstrating the effectiveness of interleaving for better feature integration and overall performance.

The performance differences between SigLIP and adapted DINOv2 highlight the varying importance of global versus localized features. For face-manipulated data like DD-VQA, where manipulations are confined to small pixel regions, DINOv2 VOM features are more effective than VLM-derived global features. Conversely, for fully synthetic data such as DVF, which requires understanding global context across the entire frame, VLM features (SigLIP) outperform VOM features. This underscores the need for a hybrid approach in TruthLens to balance both global and localized feature representations effectively.

Ablations on Adapter: We conduct a comprehensive ablation study on adapter configurations in Table 5:

1. Stage-1 trained on DD-VQA [70] & DVF [52]: The adapter is directly pretrained on DD-VQA [70] and DVF [52] datasets, with its parameters frozen during Stage-2.
2. Stage-2 frozen: The adapter is pretrained on LCS-558K [36], with its parameters frozen during Stage-2.
3. Co-trained with LLM: A single-stage training approach where the adapter and LLM are jointly trained on DD-VQA [70] and DVF [52] datasets.

These configurations are compared against our proposed two-stage approach, where the adapter is pretrained on LCS-558K [36] in Stage-1 and fine-tuned alongside the LLM in Stage-2. The results show that our approach out-

Table 6. **Ablation on data compression factors:** Results obtained by the TruthLens model on different compression factors of the FF++ [47] dataset using the same language annotations from DD-VQA [70]. The small differences across the compression factors highlight the robustness of TruthLens.

Compression	Accuracy ↑	BLEU.3 ↑	BLUE.4 ↑	ROUGE.L ↑	CIDEr ↑
raw	94.17%	0.4587	0.4131	0.6270	2.6109
c23	93.61%	0.4610	0.4269	0.6103	2.6057
c40	94.12%	0.4649	0.4304	0.6285	2.6321

performs all others, combining general-purpose pretraining with task-specific adaptation. Setting-1 fails to leverage broader multimodal understanding, Setting-2 lacks task-specific fine-tuning and Setting-3 misses general-purpose pretraining benefits. Our method balances general feature extraction with DeepFake-specific adaptation, achieving robust performance across diverse scenarios.

Ablation on Resolutions: We analyze TruthLens’s performance across different compression levels (“raw,” “c23,” and “c40”) of the FF++ dataset [47], using language annotations from DD-VQA [70]. Results in Table 6 show minimal performance variation, demonstrating TruthLens’s robustness to data compression and consistent effectiveness across varying input quality and resolution.

5. Conclusion

In this work, we introduce TruthLens, a novel and highly generalizable framework for DeepFake detection that integrates global and localized feature representations to achieve state-of-the-art performance. By combining PaliGemma2 and DINOv2 features, TruthLens effectively detects both face-manipulated and fully AI-generated content, providing detailed textual explanations for its predictions. Extensive evaluations demonstrate its robustness across diverse datasets, its ability to capture subtle inconsistencies, and distinguish between manipulated and authentic content with fine-grained reasoning. With its unified design and focus on explainability, TruthLens represents a significant step forward in building trustworthy and interpretable DeepFake detection systems.

References

- [1] Josh Achiam, Steven Adler, Sandhini Agarwal, Lama Ahmad, Ilge Akkaya, Florencia Leoni Aleman, Diogo Almeida, Janko Altenschmidt, Sam Altman, Shyamal Anadkat, et al. Gpt-4 technical report. *arXiv preprint arXiv:2303.08774*, 2023. 2, 3
- [2] Agil Aghasanli, Dmitry Kangin, and Plamen Angelov. Interpretable-through-prototypes deepfake detection for diffusion models. In *Proceedings of the IEEE/CVF international conference on computer vision*, pages 467–474, 2023. 3
- [3] Ibrahim M Alabdulmohsin, Xiaohua Zhai, Alexander Kolesnikov, and Lucas Beyer. Getting vit in shape: Scaling laws for compute-optimal model design. *Advances in Neural Information Processing Systems*, 36, 2024. 3, 4, 5
- [4] Jean-Baptiste Alayrac, Jeff Donahue, Pauline Luc, Antoine Miech, Iain Barr, Yana Hasson, Karel Lenc, Arthur Mensch, Katherine Millican, Malcolm Reynolds, et al. Flamingo: a visual language model for few-shot learning. *Advances in neural information processing systems*, 35:23716–23736, 2022. 2
- [5] Anurag Arnab, Mostafa Dehghani, Georg Heigold, Chen Sun, Mario Lučić, and Cordelia Schmid. Vivit: A video vision transformer. In *Proceedings of the IEEE/CVF international conference on computer vision*, pages 6836–6846, 2021. 7
- [6] Sarah Barrington, Matyas Bohacek, and Hany Farid. Deepspike dataset v1. 0. *arXiv preprint arXiv:2408.05366*, 2024. 1
- [7] Lucas Beyer, Andreas Steiner, André Susano Pinto, Alexander Kolesnikov, Xiao Wang, Daniel Salz, Maxim Neumann, Ibrahim Alabdulmohsin, Michael Tschannen, Emanuele Bugliarello, et al. Paligemma: A versatile 3b vlm for transfer. *arXiv preprint arXiv:2407.07726*, 2024. 7
- [8] Andreas Blattmann, Tim Dockhorn, Sumith Kulal, Daniel Mendelevitch, Maciej Kilian, Dominik Lorenz, Yam Levi, Zion English, Vikram Voleti, Adam Letts, et al. Stable video diffusion: Scaling latent video diffusion models to large datasets. *arXiv preprint arXiv:2311.15127*, 2023. 1
- [9] Junyi Cao, Chao Ma, Taiping Yao, Shen Chen, Shouhong Ding, and Xiaokang Yang. End-to-end reconstruction-classification learning for face forgery detection. In *Proceedings of the IEEE/CVF Conference on Computer Vision and Pattern Recognition*, pages 4113–4122, 2022. 6
- [10] Haoxing Chen, Yan Hong, Zizheng Huang, Zhuoer Xu, Zhangxuan Gu, Yaohui Li, Jun Lan, Huijia Zhu, Jianfu Zhang, Weiqiang Wang, et al. Demamba: Ai-generated video detection on million-scale genvideo benchmark. *arXiv preprint arXiv:2405.19707*, 2024. 2, 6, 7, 8
- [11] Yize Chen, Zhiyuan Yan, Siwei Lyu, and Baoyuan Wu. \mathcal{X}^2 -dfd: A framework for explainable and extendable deepfake detection. *arXiv preprint arXiv:2410.06126*, 2024. 2, 3, 4, 6
- [12] Zhe Chen, Weiyun Wang, Hao Tian, Shenglong Ye, Zhangwei Gao, Erfei Cui, Wenwen Tong, Kongzhi Hu, Jiapeng Luo, Zheng Ma, et al. How far are we to gpt-4v? closing the gap to commercial multimodal models with open-source suites. *Science China Information Sciences*, 67(12):220101, 2024. 2
- [13] Zhe Chen, Jiannan Wu, Wenhai Wang, Weijie Su, Guo Chen, Sen Xing, Muyan Zhong, Qinglong Zhang, Xizhou Zhu, Lewei Lu, et al. Internvl: Scaling up vision foundation models and aligning for generic visual-linguistic tasks. In *Proceedings of the IEEE/CVF Conference on Computer Vision and Pattern Recognition*, pages 24185–24198, 2024. 2
- [14] Jikang Cheng, Zhiyuan Yan, Ying Zhang, Yuhao Luo, Zhongyuan Wang, and Chen Li. Can we leave deepfake data behind in training deepfake detector? *arXiv preprint arXiv:2408.17052*, 2024. 2, 6
- [15] Kun Cheng, Xiaodong Cun, Yong Zhang, Menghan Xia, Fei Yin, Mingrui Zhu, Xuan Wang, Jue Wang, and Nannan Wang. Videoretalking: Audio-based lip synchronization for talking head video editing in the wild. In *SIGGRAPH Asia 2022 Conference Papers*, pages 1–9, 2022. 1
- [16] Jongwook Choi, Taehoon Kim, Yonghyun Jeong, Seungryul Baek, and Jongwon Choi. Exploiting style latent flows for generalizing deepfake video detection. In *Proceedings of the IEEE/CVF Conference on Computer Vision and Pattern Recognition*, pages 1133–1143, 2024. 6
- [17] Riccardo Corvi, Davide Cozzolino, Giovanni Poggi, Koki Nagano, and Luisa Verdoliva. Intriguing properties of synthetic images: from generative adversarial networks to diffusion models. In *Proceedings of the IEEE/CVF Conference on Computer Vision and Pattern Recognition*, pages 973–982, 2023. 2
- [18] Riccardo Corvi, Davide Cozzolino, Giada Zingarini, Giovanni Poggi, Koki Nagano, and Luisa Verdoliva. On the detection of synthetic images generated by diffusion models. In *ICASSP 2023-2023 IEEE International Conference on Acoustics, Speech and Signal Processing (ICASSP)*, pages 1–5. IEEE, 2023. 2
- [19] Davide Cozzolino, Giovanni Poggi, Riccardo Corvi, Matthias Nießner, and Luisa Verdoliva. Raising the bar of ai-generated image detection with clip. In *Proceedings of the IEEE/CVF Conference on Computer Vision and Pattern Recognition*, pages 4356–4366, 2024. 7
- [20] Shichao Dong, Jin Wang, Renhe Ji, Jiajun Liang, Haoqiang Fan, and Zheng Ge. Implicit identity leakage: The stumbling block to improving deepfake detection generalization. In *Proceedings of the IEEE/CVF Conference on Computer Vision and Pattern Recognition*, pages 3994–4004, 2023. 2
- [21] Alexey Dosovitskiy, Lucas Beyer, Alexander Kolesnikov, Dirk Weissenborn, Xiaohua Zhai, Thomas Unterthiner, Mostafa Dehghani, Matthias Minderer, Georg Heigold, Sylvain Gelly, et al. An image is worth 16x16 words: Transformers for image recognition at scale. In *ICLR*, 2021. 4
- [22] Deepfakes GitHub. <https://github.com/deepfakes/faceswap>, 2017. 1
- [23] FaceSwap GitHub. <https://github.com/MarekKowalski/FaceSwap/>, 2016. 1
- [24] Zhihao Gu, Yang Chen, Taiping Yao, Shouhong Ding, Jilin Li, Feiyue Huang, and Lizhuang Ma. Spatiotemporal inconsistency learning for deepfake video detection. In *Proceedings of the 29th ACM international conference on multimedia*, pages 3473–3481, 2021. 7

- [25] Xiao Guo, Xiaohong Liu, Zhiyuan Ren, Steven Grosz, Iacopo Masi, and Xiaoming Liu. Hierarchical fine-grained image forgery detection and localization. In *Proceedings of the IEEE/CVF Conference on Computer Vision and Pattern Recognition*, pages 3155–3165, 2023. 6, 7
- [26] Baojin Huang, Zhongyuan Wang, Jifan Yang, Jiabin Ai, Qin Zou, Qian Wang, and Dengpan Ye. Implicit identity driven deepfake face swapping detection. In *Proceedings of the IEEE/CVF conference on computer vision and pattern recognition*, pages 4490–4499, 2023. 6
- [27] Bin Huang, Xin Wang, Hong Chen, Zihan Song, and Wenwu Zhu. Vtimellm: Empower llm to grasp video moments. In *Proceedings of the IEEE/CVF Conference on Computer Vision and Pattern Recognition*, pages 14271–14280, 2024. 5
- [28] Shan Jia, Reilin Lyu, Kangran Zhao, Yize Chen, Zhiyuan Yan, Yan Ju, Chuanbo Hu, Xin Li, Baoyuan Wu, and Siwei Lyu. Can chatgpt detect deepfakes? a study of using multimodal large language models for media forensics. In *Proceedings of the IEEE/CVF Conference on Computer Vision and Pattern Recognition*, pages 4324–4333, 2024. 2, 3
- [29] Rohit Kundu, Hao Xiong, Vishal Mohanty, Athula Balachandran, and Amit K Roy-Chowdhury. Towards a universal synthetic video detector: From face or background manipulations to fully ai-generated content. *Proceedings of the IEEE/CVF Conference on Computer Vision and Pattern Recognition*, 2025. 2, 3
- [30] Blackforest Labs. Flux 1.1. <https://blackforestlabs.ai/>, 2024. 1
- [31] Junnan Li, Dongxu Li, Caiming Xiong, and Steven Hoi. Blip: Bootstrapping language-image pre-training for unified vision-language understanding and generation. In *International conference on machine learning*, pages 12888–12900. PMLR, 2022. 2, 3, 6
- [32] Lingzhi Li, Jianmin Bao, Hao Yang, Dong Chen, and Fang Wen. Faceshifter: Towards high fidelity and occlusion aware face swapping. *arXiv preprint arXiv:1912.13457*, 2019. 1
- [33] Y Li. Exposing deepfake videos by detecting face warping artif acts. *arXiv preprint arXiv:1811.00656*, 2018. 2
- [34] Yuezun Li, Xin Yang, Pu Sun, Honggang Qi, and Siwei Lyu. Celeb-df: A large-scale challenging dataset for deepfake forensics. In *Proceedings of the IEEE/CVF conference on computer vision and pattern recognition*, pages 3207–3216, 2020. 6, 7, 8
- [35] Yuzhen Lin, Wentang Song, Bin Li, Yuezun Li, Jiangqun Ni, Han Chen, and Qiushi Li. Fake it till you make it: Curricular dynamic forgery augmentations towards general deepfake detection. In *European Conference on Computer Vision*, pages 104–122. Springer, 2024. 6
- [36] Haotian Liu, Chunyuan Li, Qingyang Wu, and Yong Jae Lee. Visual instruction tuning. *Advances in neural information processing systems*, 36, 2024. 2, 3, 4, 5, 8
- [37] Yuqi Liu, Pengfei Xiong, Luhui Xu, Shengming Cao, and Qin Jin. Ts2-net: Token shift and selection transformer for text-video retrieval. In *European conference on computer vision*, pages 319–335. Springer, 2022. 7
- [38] Yunsheng Ni, Depu Meng, Changqian Yu, Chengbin Quan, Dongchun Ren, and Youjian Zhao. Core: Consistent representation learning for face forgery detection. In *Proceedings of the IEEE/CVF conference on computer vision and pattern recognition*, pages 12–21, 2022. 6
- [39] Ming Nie, Dan Ding, Chunwei Wang, Yuanfan Guo, Jianhua Han, Hang Xu, and Li Zhang. Slowfocus: Enhancing fine-grained temporal understanding in video llm. In *The Thirty-eighth Annual Conference on Neural Information Processing Systems*, 2024. 5
- [40] Utkarsh Ojha, Yuheng Li, and Yong Jae Lee. Towards universal fake image detectors that generalize across generative models. In *Proceedings of the IEEE/CVF Conference on Computer Vision and Pattern Recognition*, pages 24480–24489, 2023. 2, 7
- [41] Maxime Oquab, Timothée Darcet, Théo Moutakanni, Huy Vo, Marc Szafraniec, Vasil Khalidov, Pierre Fernandez, Daniel Haziza, Francisco Massa, Alaaeldin El-Nouby, et al. Dinov2: Learning robust visual features without supervision. *arXiv preprint arXiv:2304.07193*, 2023. 2, 4, 5, 7
- [42] Tianshuo Peng, Zuchao Li, Lefei Zhang, Hai Zhao, Ping Wang, and Bo Du. Multi-modal auto-regressive modeling via visual tokens. In *Proceedings of the 32nd ACM International Conference on Multimedia*, page 10735–10744, New York, NY, USA, 2024. Association for Computing Machinery. 5
- [43] KR Prajwal, Rudrabha Mukhopadhyay, Vinay P Namboodiri, and CV Jawahar. A lip sync expert is all you need for speech to lip generation in the wild. In *Proceedings of the 28th ACM international conference on multimedia*, pages 484–492, 2020. 1
- [44] Yuyang Qian, Guojun Yin, Lu Sheng, Zixuan Chen, and Jing Shao. Thinking in frequency: Face forgery detection by mining frequency-aware clues. In *European conference on computer vision*, pages 86–103. Springer, 2020. 7
- [45] Alec Radford, Jong Wook Kim, Chris Hallacy, Aditya Ramesh, Gabriel Goh, Sandhini Agarwal, Girish Sastry, Amanda Askell, Pamela Mishkin, Jack Clark, et al. Learning transferable visual models from natural language supervision. In *International conference on machine learning*, pages 8748–8763. PmLR, 2021. 2
- [46] Runway Research. Text driven video generation. <https://research.runwayml.com/gen2>, 2023. 1
- [47] Andreas Rossler, Davide Cozzolino, Luisa Verdoliva, Christian Riess, Justus Thies, and Matthias Nießner. Faceforensics++: Learning to detect manipulated facial images. In *Proceedings of the IEEE/CVF international conference on computer vision*, pages 1–11, 2019. 1, 3, 6, 8
- [48] Henry Ruhs. Facefusion, 2024. 1
- [49] Zeyang Sha, Zheng Li, Ning Yu, and Yang Zhang. De-fake: Detection and attribution of fake images generated by text-to-image generation models. In *Proceedings of the 2023 ACM SIGSAC Conference on Computer and Communications Security*, pages 3418–3432, 2023. 7
- [50] Yichen Shi, Yuhao Gao, Yingxin Lai, Hongyang Wang, Jun Feng, Lei He, Jun Wan, Changsheng Chen, Zitong Yu, and Xiaochun Cao. Shield: An evaluation benchmark for face spoofing and forgery detection with multimodal large language models. *arXiv preprint arXiv:2402.04178*, 2024. 2, 3

- [51] Kaede Shiohara and Toshihiko Yamasaki. Detecting deepfakes with self-blended images. In *Proceedings of the IEEE/CVF conference on computer vision and pattern recognition*, pages 18720–18729, 2022. 6
- [52] Xiufeng Song, Xiao Guo, Jiache Zhang, Qirui Li, Lei Bai, Xiaoming Liu, Guangtao Zhai, and Xiaohong Liu. On learning multi-modal forgery representation for diffusion generated video detection. *The Thirty-eighth Annual Conference on Neural Information Processing Systems*, 2024. 1, 2, 3, 4, 6, 7, 8
- [53] Andreas Steiner, André Susano Pinto, Michael Tschannen, Daniel Keysers, Xiao Wang, Yonatan Bitton, Alexey Gritsenko, Matthias Minderer, Anthony Sherbondy, Shangbang Long, et al. Paligemma 2: A family of versatile vlms for transfer. *arXiv preprint arXiv:2412.03555*, 2024. 1, 2, 3, 4, 5, 7
- [54] Ke Sun, Shen Chen, Taiping Yao, Hong Liu, Xiaoshuai Sun, Shouhong Ding, and Rongrong Ji. Diffusionfake: Enhancing generalization in deepfake detection via guided stable diffusion. *NeurIPS*, 2024. 2
- [55] Chuangchuang Tan, Yao Zhao, Shikui Wei, Guanghua Gu, Ping Liu, and Yunchao Wei. Rethinking the up-sampling operations in cnn-based generative network for generalizable deepfake detection. In *Proceedings of the IEEE/CVF Conference on Computer Vision and Pattern Recognition*, pages 28130–28139, 2024. 7
- [56] Gemini Team, Rohan Anil, Sebastian Borgeaud, Jean-Baptiste Alayrac, Jiahui Yu, Radu Soricut, Johan Schalkwyk, Andrew M Dai, Anja Hauth, Katie Millican, et al. Gemini: a family of highly capable multimodal models. *arXiv preprint arXiv:2312.11805*, 2023. 2, 3, 6
- [57] Gemma Team, Morgane Riviere, Shreya Pathak, Pier Giuseppe Sessa, Cassidy Hardin, Surya Bhupatiraju, Léonard Hussenot, Thomas Mesnard, Bobak Shahriari, Alexandre Ramé, et al. Gemma 2: Improving open language models at a practical size. *arXiv preprint arXiv:2408.00118*, 2024. 3, 4, 5
- [58] Justus Thies, Michael Zollhöfer, and Matthias Nießner. Deferred neural rendering: Image synthesis using neural textures. *Acm Transactions on Graphics (TOG)*, 38(4):1–12, 2019. 1
- [59] Shengbang Tong, Zhuang Liu, Yuexiang Zhai, Yi Ma, Yann LeCun, and Saining Xie. Eyes wide shut? exploring the visual shortcomings of multimodal llms. In *Proceedings of the IEEE/CVF Conference on Computer Vision and Pattern Recognition*, pages 9568–9578, 2024. 2, 4
- [60] Jiuniu Wang, Hangjie Yuan, Dayou Chen, Yingya Zhang, Xiang Wang, and Shiwei Zhang. Modelscope text-to-video technical report. *arXiv preprint arXiv:2308.06571*, 2023. 1
- [61] Sheng-Yu Wang, Oliver Wang, Richard Zhang, Andrew Owens, and Alexei A Efros. Cnn-generated images are surprisingly easy to spot... for now. In *Proceedings of the IEEE/CVF conference on computer vision and pattern recognition*, pages 8695–8704, 2020. 7
- [62] Zhendong Wang, Jianmin Bao, Wengang Zhou, Weilun Wang, Hezhen Hu, Hong Chen, and Houqiang Li. Dire for diffusion-generated image detection. In *Proceedings of the IEEE/CVF International Conference on Computer Vision*, pages 22445–22455, 2023. 2, 7
- [63] Ying Xu, Kiran Raja, and Marius Pedersen. Supervised contrastive learning for generalizable and explainable deepfakes detection. In *Proceedings of the IEEE/CVF Winter Conference on Applications of Computer Vision*, pages 379–389, 2022. 3
- [64] Yuting Xu, Jian Liang, Gengyun Jia, Ziming Yang, Yanhao Zhang, and Ran He. Tall: Thumbnail layout for deepfake video detection. In *Proceedings of the IEEE/CVF international conference on computer vision*, pages 22658–22668, 2023. 2, 6, 7
- [65] Zhiyuan Yan, Yong Zhang, Yanbo Fan, and Baoyuan Wu. Ucf: Uncovering common features for generalizable deepfake detection. In *Proceedings of the IEEE/CVF International Conference on Computer Vision*, pages 22412–22423, 2023. 6
- [66] Zhiyuan Yan, Yuhao Luo, Siwei Lyu, Qingshan Liu, and Baoyuan Wu. Transcending forgery specificity with latent space augmentation for generalizable deepfake detection. In *Proceedings of the IEEE/CVF Conference on Computer Vision and Pattern Recognition*, pages 8984–8994, 2024. 6
- [67] Zhiyuan Yan, Taiping Yao, Shen Chen, Yandan Zhao, Xinghe Fu, Junwei Zhu, Donghao Luo, Li Yuan, Chengjie Wang, Shouhong Ding, et al. Df40: Toward next-generation deepfake detection. *NeurIPS* 2024, 2024. 6, 7, 8
- [68] Xin Yang, Yuezun Li, and Siwei Lyu. Exposing deep fakes using inconsistent head poses. In *ICASSP 2019-2019 IEEE International Conference on Acoustics, Speech and Signal Processing (ICASSP)*, pages 8261–8265. IEEE, 2019. 2
- [69] Renrui Zhang, Jiaming Han, Chris Liu, Aojun Zhou, Pan Lu, Yu Qiao, Hongsheng Li, and Peng Gao. Llama-adapter: Efficient fine-tuning of large language models with zero-initialized attention. In *The Twelfth International Conference on Learning Representations*, 2024. 2
- [70] Yue Zhang, Ben Colman, Xiao Guo, Ali Shahriyari, and Gaurav Bharaj. Common sense reasoning for deepfake detection. In *European Conference on Computer Vision*, pages 399–415. Springer, 2024. 2, 3, 4, 6, 7, 8
- [71] Cairong Zhao, Chutian Wang, Guosheng Hu, Haonan Chen, Chun Liu, and Jinhui Tang. Istvt: interpretable spatial-temporal video transformer for deepfake detection. *IEEE Transactions on Information Forensics and Security*, 18: 1335–1348, 2023. 6
- [72] Zangwei Zheng, Xiangyu Peng, Tianji Yang, Chenhui Shen, Shenggui Li, Hongxin Liu, Yukun Zhou, Tianyi Li, and Yang You. Open-sora: Democratizing efficient video production for all, 2024. 1
- [73] Deyao Zhu, Jun Chen, Xiaoqian Shen, Xiang Li, and Mohamed Elhoseiny. Minigpt-4: Enhancing vision-language understanding with advanced large language models. *arXiv preprint arXiv:2304.10592*, 2023. 2
- [74] Dragoș-Constantin Țânțaru, Elisabeta Oneață, and Dan Oneață. Weakly-supervised deepfake localization in diffusion-generated images. In *Proceedings of the IEEE/CVF Winter Conference on Applications of Computer Vision*, pages 6258–6268, 2024. 3